European Journal of Radiology 112 (2019) 144–152

Contents lists available at ScienceDirect

European Journal of Radiology

journal homepage: www.elsevier.com/locate/ejrad

Diffusion kurtosis imaging histogram parameter metrics predicting survival in integrated molecular subtypes of diffuse glioma: An observational cohort study

Johann-Martin Hempel[a,f,*], Cornelia Brendle[a,f], Benjamin Bender[a,f], Georg Bier[a,f], Mareen Sarah Kraus[a], Marco Skardelly[b,c,f], Hardy Richter[c], Franziska Eckert[d,f], Jens Schittenhelm[e,f], Ulrike Ernemann[a,f], Uwe Klose[a]

[a] Department of Neuroradiology, University Hospital Tübingen, Eberhard Karls University, Tübingen, Germany
[b] Department of Neurosurgery, University Hospital Tübingen, Eberhard Karls University, Tübingen, Germany
[c] Interdisciplinary Division of Neuro-Oncology, Departments of Neurology and Neurosurgery, University Hospital Tübingen, Hertie Institute for Clinical Brain Research, Eberhard Karls University, Tübingen, Germany
[d] Department of Radiation Oncology, University Hospital Tübingen, Eberhard Karls University, Tübingen, Germany
[e] Institute of Neuropathology, Department of Pathology and Neuropathology, University Hospital Tübingen, Eberhard Karls University, Tübingen, Germany
[f] Center for CNS Tumors, Comprehensive Cancer Center Tübingen-Stuttgart, University Hospital Tübingen, Eberhard Karls University, Tübingen, Germany

ARTICLE INFO

Keywords:
Glioma
Diffusion kurtosis imaging
Mean kurtosis
Mean diffusivity
Survival
Prognosis

ABSTRACT

Purpose: The aim of the study was to assess the predictive value of preoperatively assessed diffusion kurtosis imaging (DKI) metrics as prognostic factors in the 2016 World Health Organization Classification of Tumors of the Central Nervous System integrated glioma groups.

Material and methods: Seventy-seven patients with histopathologically confirmed treatment-naïve glioma were retrospectively assessed between 08/2013 and 10/2017 using mean kurtosis (MK) and mean diffusivity (MD) histogram parameters from DKI, overall and progression-free survival, and relevant prognostic molecular data (isocitrate dehydrogenase, [IDH]; alpha-thalassemia/mental retardation syndrome X-linked, [ATRX]; chromosome 1p/19q loss of heterozygosity). Receiver operating characteristic (ROC) analysis was performed on metric variables to determine the optimal cutoff-values. The Kaplan-Meier method was used to assess univariate survival data. A multivariate Cox proportional hazards model was performed on significant results from the univariate analysis.

Results: There were significant differences in overall and progression-free survival between patient age ($p = 0.001$), resection statuses ($p = 0.002$), WHO glioma grades ($p < 0.0001$), and integrated molecular profiles ($p < 0.0001$). Survival was significantly better in patients with lower MK and higher MD values globally ($p = 0.009$), in gliomas without chromosome 1p/19q LOH ($p < 0.0001$), and those with retained ATRX expression ($p = 0.008$).

Conclusions: Patient age and MK from DKI from DKI are relevant factors for preoperatively predicting overall and progression-free survival. Regarding the molecular subgroups, they seem to be predictive in gliomas with ATRX retention, representing a feature of IDH wild-type gliomas.

1. Introduction

Gliomas are the most common intrinsic brain tumors with a worldwide incidence of 6/100.000 [1]. They are associated with poor prognosis and substantial morbidity [2]. Properly determining glioma characteristics has an impact on clinical management and individual prognosis [3]. For final glioma grading the histopathological examination is indispensable [4,5]. The recently updated World Health Organization classification (revised 4th edition) of tumors of the central nervous system (2016 CNS WHO) joins both histopathological and molecular features into an “integrated diagnosis” thus establishing new tumor subclasses [3]. For appraising individual prognosis, the molecular stratification is essential and also superior to conventional histological grading [6–8]. In reference to 2016 CNS WHO the basic

* Corresponding author at: Department of Neuroradiology, University Hospital Tübingen, Eberhard Karls University, Tübingen, Germany.
E-mail address: johann-martin.hempel@uni-tuebingen.de (J.-M. Hempel).

https://doi.org/10.1016/j.ejrad.2019.01.014
Received 19 September 2018; Received in revised form 22 November 2018; Accepted 14 January 2019
0720-048X/

molecular characteristics include isocitrate-dehydrogenase (IDH) 1/2 mutation status and chromosome 1p/19q loss of heterozygosity (LOH). Both mutation of IDH1/2 and chromosome 1p/19q LOH are favorable prognostic factors in diffuse glioma [6–12]. Alpha-thalassemia/mental retardation syndrome X-linked (ATRX) is a complementary molecular marker, which is predictive for associated IDH or H3 histone, family 3 A (H3F3 A) hotspot mutations [13]. The loss of ATRX expression is mostly induced by truncating ATRX mutations, resulting in an alternative lengthening of telomeres (ALT) phenotype [14]. It also represents a favorable prognostic factor in diffuse glioma [11]. The O6-methylguanine DNA methyltransferase (MGMT) methylation status is an independent prognostic factor in diffuse glioma [15–17]. However, non-invasive multi-modal imaging methods are essential for post-treatment monitoring of potential tumor recurrence, for follow-up of patients with suspected low-grade glioma or those not being eligible for surgery, or for reliable in-vivo glioma characterization in patients with an increased risk of post-biopsy complications [18].

The apparent diffusional kurtosis — also known as the apparent kurtosis coefficient (AKC) — is a dimensionless metric from diffusion kurtosis imaging (DKI) that quantifies the degree of deviation from Gaussian diffusion behavior of the diffusion induced signal decay [19–21]. DKI is an extension of the diffusion tensor imaging (DTI) method that uses multiple and high b-value measurements in multiple directions [19–24]. The metrics that can be derived from DKI are the mean kurtosis (MK) and mean diffusivity (MD) [24,21]. DKI allows for quantitative assessment of the water diffusion behavior in a biological tissue that goes beyond that of mono-exponential apparent diffusion coefficient (ADC) measurements from standard single b-value diffusion weighted imaging (DWI). However, diffusion barriers change the water diffusion probability distribution of a biological tissue such as brain tissue. Regarding the high anisotropy of brain tissue, DKI can be regarded as a measure of its microstructural composition, heterogeneity, and complexity [19,22]. Previously, DKI has shown potential in non-invasively discriminating between 2016 CNS WHO glioma grades and their integrated molecular profiles [25,26].

However, the prognostic value of MK and MD parameters from DKI on pre-treatment MRI images in view of integrated “histo-molecular” tumor stratification has not yet been investigated. Therefore, this study sought to assess the predictive value of MK and MD parameters from DKI on preoperative MR images as prognostic factors in 2016 CNS WHO integrated glioma groups.

2. Material and methods

2.1. Study design and ethics

This study is a retrospective observational cohort analysis according to the STROBE guidelines [27], and it was conducted based on the principles of the International Conference on Harmonization: Good Clinical Practice guidelines and the latest version of the Declaration of Helsinki. The local institutional review board approved this study (Ref. No. 727/2017BO2) and waived the written informed consent due to the retrospective study design.

2.2. Patient selection and stratification

The patient cohort was selected from 397 consecutive patients with diffuse glioma diagnoses from 08/2013 and 10/2017. Fig. 1 demonstrates the patient selection and dichotomization algorithm using a flow diagram. The final study group comprised 77 patients with a mean age of 53.1 ± 15.7 years and consisted of 43 men (56%) and 34 women (44%). The mean follow-up time was 534 days (1.46 years) with a range of 30–1738 days (0–4.76 years). Glioma grading was based on histopathological examinations and full immunohistochemical work-up of specimens obtained from partial, subtotal (> 90%), or complete tumor resection in all patients, whereas several patients underwent prior navigated biopsy.

Immunohistochemistry with a mutation-specific IDH1 R132H antibody assessed the IDH mutation status [28]. The negative cases followed Sanger sequencing to detect any non-canonical IDH1/2 mutations [29]. Immunohistochemistry also determined nuclear ATRX expression status in tumor cells using cut-off values as previously [13]. Chromosome 1p/19q LOH was studied using a synthetic high-resolution microsatellite polymerase chain reaction (PCR) gel [30]. All high-grade tumors underwent assessment of MGMT methylation by methylation-specific PCR [15,31].

Final glioma classification was based on the current 2016 CNS WHO criteria [3] and included both histopathological and molecular data. In the integrated approach the combination of loss of ATRX expression and presence of IDH1/2 mutation characterized IDH_{mut} astrocytoma (AS) including its most aggressive histological subtype of IDH_{mut} glioblastoma (GBM). Tumors with IDH wild type (IDH_{WT}) status and retained ATRX expression are primary GBMs. Oligodendrogliomas are defined by synchronous 1p/19q LOH and IDH1/2 mutation, whereas an overwhelming majority are associated with maintained ATRX expression [1,7,30]. Additionally, IDH_{mut} diffuse AS WHO grade II (AS2), IDH_{mut} anaplastic AS WHO grade III (AS3), and IDH_{mut} AS4/GBMs WHO grade IV were grouped as (1) IDH_{mut} AS; IDH_{wt} AS2, IDH_{wt} AS3, and IDH_{wt} AS4/GBM were grouped as (2) IDH_{wt} GBM, and 1p/19q-confirmed diffuse (OD2) and anaplastic oligodendrogliomas (OD3) were grouped as (3) $OD_{1p/19q\text{-}LOH}$ based on their integrated molecular profiles as well as their clinical outcomes [6,7,11,12].

2.3. Procedures and techniques

2.3.1. MR imaging

Imaging used a 3.0 T MRI scanner (Biograph mMR, Siemens Healthcare, Erlangen, Germany) with a 32-channel head coil. The conventional MR examination protocol included a transversal 2D-encoded T2-weighted fluid attenuated inversion recovery (FLAIR) sequence (TR/TE, 9000/87 ms; inversion time (TI), 2500 ms; slice number, 40; slice thickness, 3 mm), and a sagittal 3D-encoded isotropic magnetization prepared rapid acquisition gradient echo (MPRAGE) sequence (TR/TE, 1900/2.4 ms; TI, 900 ms; slice number, 124; slice thickness, 1.0 mm) before and after administration of 0.1 ml/kg body weight gadobutrol (Gadovist®, Bayer, Leverkusen, Germany).

For DKI, a spin-echo 2D echo-planar imaging diffusion-weighted imaging (DWI) sequence was used. The implemented b-values were 0, 500, 1000, 1500, 2000, and 2500s/mm^2. Diffusion encoding in 30 directions was used for each of these values. The other imaging parameters included: TR, 5900 ms; TE, 95 ms; field of view, 250 × 250 mm^2; matrix, 128 × 128; slice number, 25; slice thickness, 5 mm; bandwidth, 965 Hz/pixel; and parallel imaging with a sensitivity encoding factor of 2 in the anteroposterior direction.

2.3.2. Image post-processing and analysis

As previously described [25], MD and MK parametric maps were calculated, and smoothing was applied prior to calculation of the parametric maps using the MR Body Diffusion tool® V.1.2.0 in syngo.via frontier® (Siemens Healthcare, Erlangen, Germany). Image and volume of interest (VOI) analyses were performed on the parametric maps using MIPAV 7.4.0 (http://mipav.cit.nih.gov/). The entire tumor volume was manually delineated around the most solid-appearing parts of each whole tumor on multiple slices, as indicated by T2 signal alterations. Necrotic areas, greater vessels, and peritumoral edema were excluded. By encompassing the whole tumor volume potential sampling bias was minimized [32,33]. The MD and MK parametric maps were then transformed on the matrix of the transverse FLAIR-weighted images using in-house Matlab-based software (Matlab 2014b, MathWorks Natick, Massachusetts, USA). Subsequently, the MK and MD voxel intensity values were extracted voxel-wise from the overlaid VOIs and exported for statistical analysis.

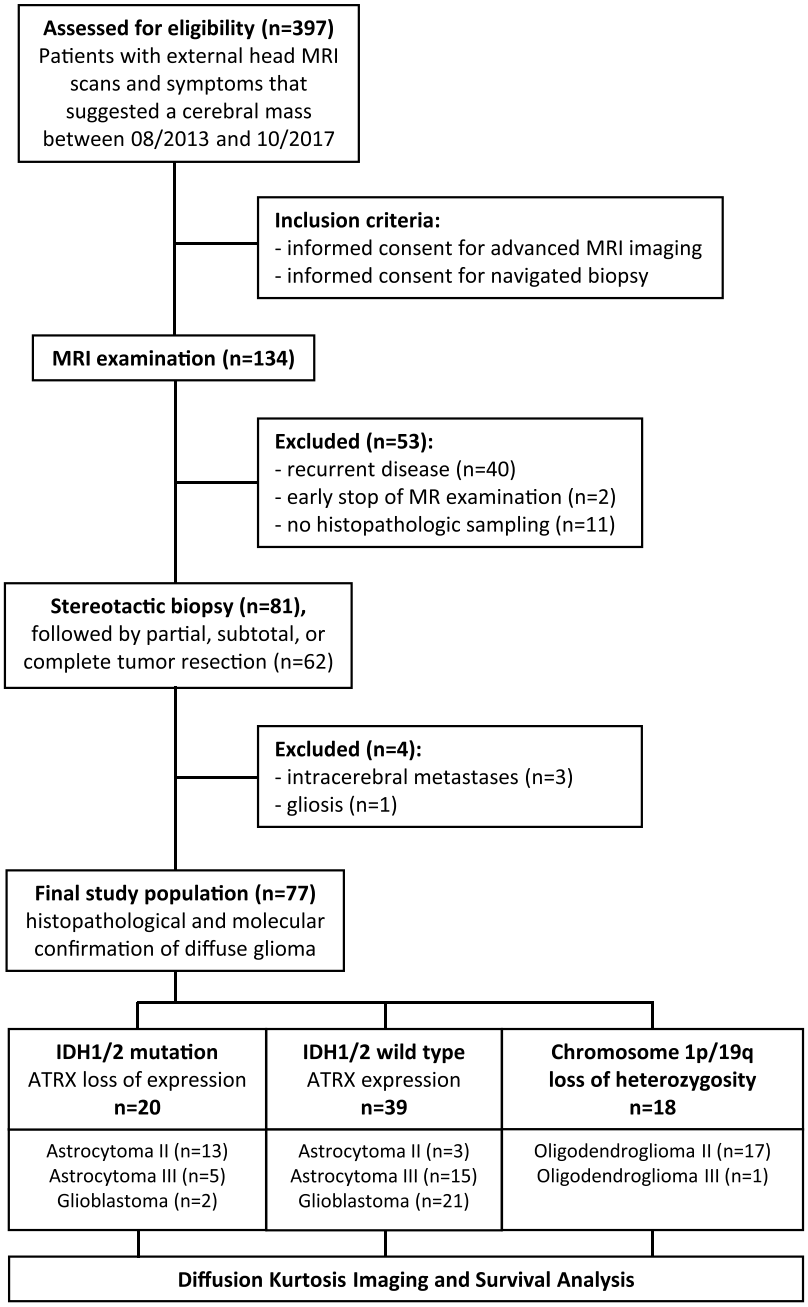

Fig. 1. Patient flow diagram according to the STROBE guidelines.

The following ten standard first-order parameters were derived from the MK and MD histograms: mean, mode (equals the peak height position), standard deviation (SD), skewness (measure of the asymmetry of a distribution), kurtosis (degree of "tailedness" of a distribution) as well as the tenth (C10), 25th (C25), 50th (C50), 75th (C75), and 90th (C90) percentiles.

2.3.3. Statistical analyses

Data analyses were performed using IBM SPSS Statistics® Version 24 (IBM, Armonk, NY, USA) and validated using JMP 13.1 (SAS, Discovery, Cary, NJ, USA). Receiver operating characteristic (ROC) curves were generated for significant results to determine the optimal cutoff-values from metric variables such as MD, MK, and age. These cutoff-values were globally applied to following analyses. The Kaplan-Meier method and the Tarone-Ware test [34,35] were used to assess univariate survival data among the different subgroups (resection status, WHO grade, integrated molecular profiles, IDH1/2 mutation status, ATRX expression status, and age; see Figs. 2 and 3). They were also used to assess univariate survival data between different MK and MD values among the different subgroups (Figs. 4 and 5). Multivariate survival analysis was performed using the Cox proportional hazards regression model. Regarding the aim of the study, only preoperatively known parameters such as age or DKI parameters, which showed significant results from univariate analysis, were included into multivariate analysis (Table 4). The hazard ratios corresponded to risk of death, and thus, an increased hazard ratio implied an unfavorable prognosis. Due to multicollinearity in DKI histogram parameters only the most significant parameter from univariate analysis (average MK) was included into multivariate analysis. The global level of significance was set at $\alpha = 0.05$.

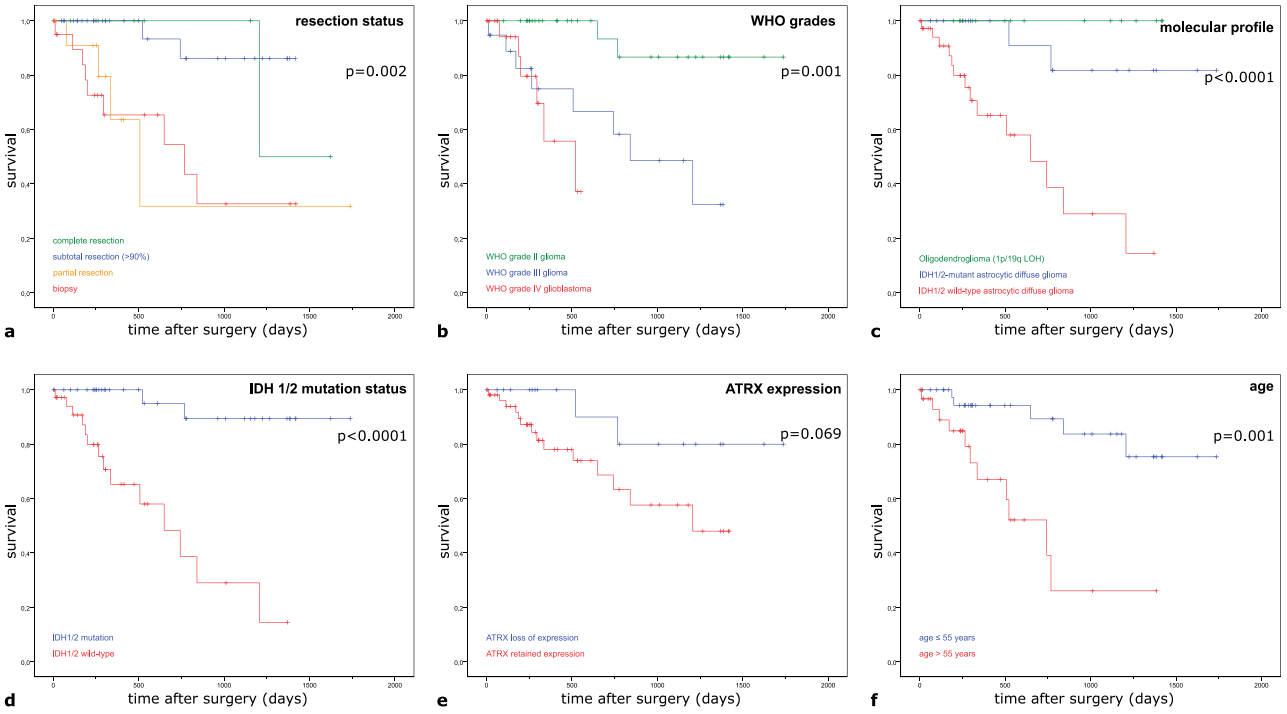

Fig. 2. Overall survival among glioma subgroups Kaplan-Meier plots illustrating overall patient survival among different resection statuses (a), WHO grades (b), integrated molecular profiles (c), IDH1/2 mutation status (d), ATRX expression status (e), and age groups (f). WHO, world health organization; IDH1/2, isocitrate dehydrogenase 1/2; ATRX, alpha-thalassemia/mental retardation syndrome X-linked; MGMT, O6-methylguanine DNA methyltransferase.

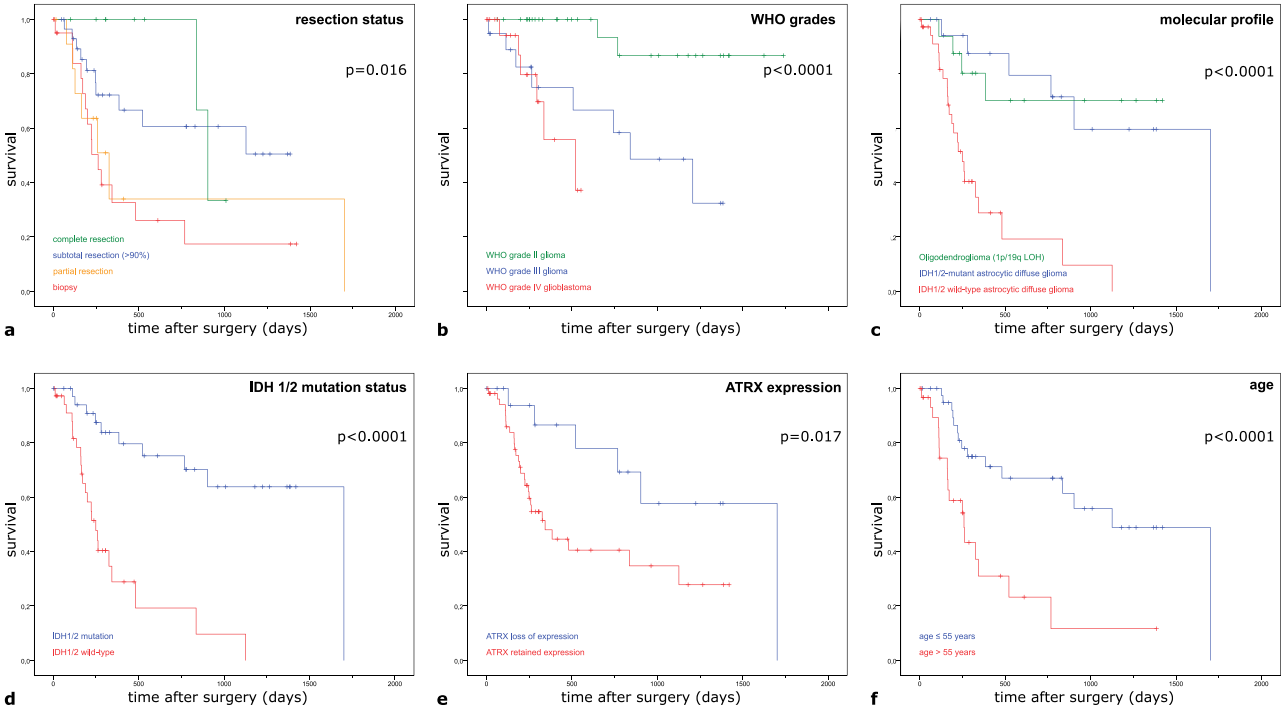

Fig. 3. Progression-free survival among glioma subgroups Kaplan-Meier plots illustrating progression-free patient survival among different resection statuses (a), WHO grades (b), integrated molecular profiles (c), IDH1/2 mutation status (d), ATRX expression status (e), and age groups (f). WHO, world health organization; IDH1/2, isocitrate dehydrogenase 1/2; ATRX, alpha-thalassemia/mental retardation syndrome X-linked; MGMT, O6-methylguanine DNA methyltransferase.

3. Results

3.1. Descriptive statistics

Tables 1 and 2 show the distribution of the histopathological and molecular characteristics according to 2016 CNS WHO as well as the grouped findings based on their integrated molecular profiles and clinical outcomes [6,7,11,12]. The tables comprise descriptive survival data among the different histopathological and molecular subgroups. The overall mean survival was 3.42 years. The mean and median progression-free survival were 2.3 and 2.1 years, respectively.

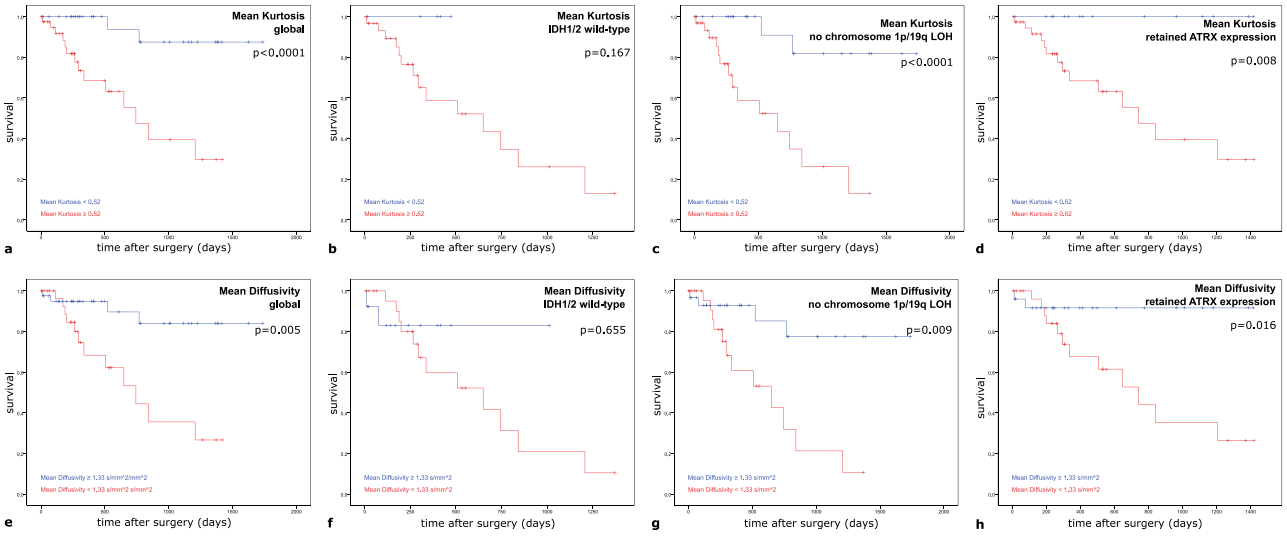

Fig. 4. Overall survival data for Mean Kurtosis and Mean Diffusivity from Diffusion Kurtosis Imaging among glioma subgroups Kaplan-Meier plots illustrating overall patient survival between different MK (a) and MD values (e) among the integrated glioma groups of IDH_{wt} GBM (b, f), gliomas without chromosome 1p/19q LOH (c, g), and gliomas with retained expression (d, h).
IDH1/2, isocitrate dehydrogenase 1/2; IDH_{mut}, IDH-mutant; IDH_{wt}, IDH wild type; $OD_{1p/19q\text{-}LOH}$, oligodendroglioma with chromosome 1p/19q loss of heterozygosity; ATRX, alpha-thalassemia/mental retardation syndrome X-linked

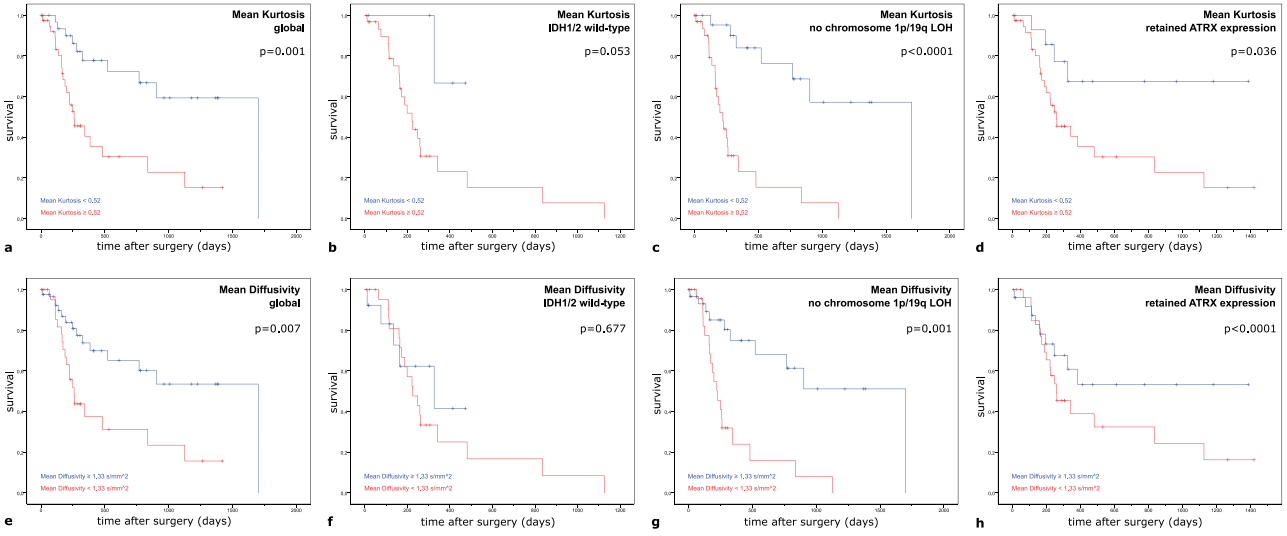

Fig. 5. Progression-free survival data for Mean Kurtosis and Mean Diffusivity from Diffusion Kurtosis Imaging among glioma subgroups Kaplan-Meier plots illustrating progression-free patient survival between different MK (a) and MD values (e) among the integrated glioma groups of IDH_{wt} GBM (b, f), gliomas without chromosome 1p/19q LOH (c, g), and gliomas with retained expression (d, h).
IDH1/2, isocitrate dehydrogenase 1/2; IDH_{mut}, IDH-mutant; IDH_{wt}, IDH wild type; $OD_{1p/19q\text{-}LOH}$, oligodendroglioma with chromosome 1p/19q loss of heterozygosity; ATRX, alpha-thalassemia/mental retardation syndrome X-linked

3.2. Univariate survival analysis

Table 3 shows univariate survival data from Cox proportional hazards analysis. Univariate survival data from all patients is presented using the Kaplan-Meier plots and their corresponding p values from the Tarone-Ware tests (see Figs. 2, 3, 4, and 5). Regarding overall survival, there were significant differences between the different resection statuses ($p = 0.002$), WHO glioma grades ($p = 0.001$), integrated molecular profiles ($p < 0.0001$), IDH1/2 mutation status ($p < 0.0001$), and patient age group ($p = 0.001$; Fig. 2a–d; f). For progression-free survival, there were significant differences between resection statuses ($p = 0.016$), WHO glioma grades ($p < 0.0001$), integrated molecular profiles ($p < 0.0001$), IDH1/2 mutation status ($p < 0.0001$), ATRX expression status ($p = 0.017$), and patient age group ($p < 0.0001$; Fig. 3a–f).

Globally, overall and progression-free survival was significantly better in patients with lower MK values ($p < 0.0001$, Fig. 4a; $p = 0.001$, Fig. 5a) and higher MD values ($p = 0.005$, Fig. 4e; $p = 0.007$, Fig. 5e), respectively.

In the molecular groups of IDH_{mut} AS, IDH_{wt} GBM, and $OD_{1p/19q\text{-}LOH}$ there were no significant differences in overall and progression-free survival between patients with high or low MD and MK. Additionally, there were no significant differences in overall and progression-free survival between patients with high or low MD and MK values among different IDH1/2 status (Figs. 4b, f and 5 b, f). However, patients with lower MK and higher MD showed significantly better overall and progression-free survival among the group of gliomas without chromosome 1p/19q LOH (Figs. 4c, g and 5 c, g) and those with retained ATRX expression independent of IDH mutation status (Figs. 4d, h and 5 d, h).

Table 1
Tumor grading and survival data according to the 2016 CNS WHO criteria.

Histopathological characteristics								
Histology	astrocytoma		GBM	astrocytoma		GBM	oligodendroglioma	
WHO grade	II	III	IV	II	III	IV	II	III
Molecular characteristics								
IDH1/2 mutation	yes			no			yes	
1p/19q Co-Deletion	no			no			yes	
N	13	5	2	3	15	21	17	1
Age (mean/median)	40/38	43/40	53/53	53/42	56/56	63/54	51/52	18/18
Sex (male/female)	8/5	3/2	1/1	2/1	7/8	14/7	7/10	1/0
ATRX loss of expression (y/n)	13/0	4/1	2/0	0/3	0/15	1/20	0/17	0/1
MGMT promoter methylation*	4/2	2/3	0/2	1/1	4/11	8/13	1/0	0/1
Progression of disease (y/n)	3/10	1/4	2/0	1/2	11/4	12/9	4/13	1/0
Mean / median progression-free survival [years]	3.9/4.7	3.1/2.5	1.1/0.8	1.1/–	1.1/0.7	0.6/0.5	2.9/–	–
Patients deceased (y/n)	1/12	0/5	1/1	1/2	8/7	5/16	0/17	1/0
Mean / median overall survival [years]	4.4/–	–	1.4/–	1.8/–	2.0/0.6	1.1/–	–	–

GBM, glioblastoma; Isocitrate-dehydrogenase (IDH) 1/2 mutation status; alpha-thalassemia/mental retardation syndrome X-linked (ATRX) loss of expression; chromosome 1p/19q co-deletion; O6-methylguanine DNA methyltransferase (MGMT) promoter methylation status;
*Only cases with a clear-cut MGMT promoter status (methylated or unmethylated) are listed.

Table 2
Tumor grading and survival data according to the grouped findings of the integrated molecular approach.

Histopathological characteristics			
Histology	AS & GBM	AS & GBM	oligodendroglioma
WHO grade	all	all	All
Molecular characteristics			
IDH1/2 mutation	yes	no	yes
1p/19q Co-Deletion	no	no	yes
N	20	39	18
Age (mean/median)	42/39	57/59	49/51
Sex (male/female)	12/8	23/16	8/10
ATRX loss of expression (y/n)	19/1	1/38	0/18
MGMT promoter methylation*	6/7	13/25	1/1
Progression of disease (y/n)	6/14	24/15	5/13
Mean / median progression-free survival [years]	3.4/4.7	1.0/0.7	2.9/0.7
Patients deceased (y/n)	2/18	14/25	1/17
Mean / median overall survival [years]	4.2/–	1.9/1.8	–

AS, astrocytoma; GBM, glioblastoma; Isocitrate-dehydrogenase (IDH) 1/2 mutation status; alpha-thalassemia/mental retardation syndrome X-linked (ATRX) loss of expression; chromosome 1p/19q co-deletion; O6-methylguanine DNA methyltransferase (MGMT) promoter methylation status;
*Only cases with a clear-cut MGMT promoter status (methylated or unmethylated) are listed.

3.3. Multivariate survival analysis

Table 4 lists results from multivariate Cox proportional hazards analysis results from preoperatively known variables such as age and DKI parameters, which were significant in univariate analysis. Both age and average MK are significant both for overall and progression-free survival.

4. Discussion

The aim of this study was to assess the predictive value of MK and MD parameters from DKI on preoperative MR images as prognostic factors in 2016 CNS WHO integrated glioma groups. In univariate analysis, higher MK and lower MD values itself were factors for unfavorable overall and progression-free survival. Among the different subgroups, higher MK and lower MD were factors for unfavorable survival in the group of gliomas without chromosome 1p/19q LOH and those with retained ATRX expression. Also, they are relevant for predicting survival in preoperative setting in multivariate analysis.

Regarding the integrated approach of 2016 CNS WHO MK has demonstrated similar microstructure and heterogeneity within the groups of gliomas classified as IDH_{mut} AS, IDH_{wt} GBM, and $OD_{1p/19q\text{-}LOH}$ based on their molecular profile, clinical outcome, and prognosis, and irrespective of their individual WHO grades [26]. Specifically, lower MK and higher MD values correlate with the group of IDH_{mut} AS which is characterized by lower cell density and more homogeneous cell architecture than their wild-type counterpart. Conversely, the group of IDH_{wt} GBM is associated with higher MK and lower MD values due to increased cellularity, structural heterogeneity, microvascular proliferation, hemorrhage, and necrosis [25,36,37]. The group of $OD_{1p/19q\text{-}LOH}$ that shares IDH mutation with IDH_{mut} AS and retained ATRX expression with IDH_{wt} GBM, shows intermediate DKI parameters [25]. The prognostic value of DKI, which reflects the degree of morphologic complexity of a tumor, may be explained by its capability of non-invasively appraising the molecular glioma profiles, which again are associated with different survival characteristics.

5. Survival analysis

Molecular stratification is essential for estimating individual prognosis in patients with glioma [6–8]. In our study we found that younger patient age and IDH1/2 mutation are positive prognostic factors both in univariate and multivariate analysis. These results confirm various studies in the literature [6–8,38,39,10]. Regarding the integrated molecular profiles of IDH_{mut} AS, $OD_{1p/19q\text{-}LOH}$, and IDH_{wt} GBM [6,7,11,12], we found survival curves (Figs. 2c and 3c) similar to Pekmezci et al. [11], Olar et al. [10] and Hempel et al. [40], thus supporting the validity of our data and confirming the favorable prognostic value of IDH mutation and chromosome 1p/19q LOH.

The ADC from single b-value DWI on preoperative MRI images is a commonly known prognostic factor for overall survival in previous 2007 CNS WHO glioma grades [41,42]. However, the predictive value of advanced DWI parameters such as MK and MD from DKI have not yet been assessed in the literature. Regarding MK and MD alone, our data shows significantly better overall and progression-free survival in patients with lower MK and higher MD values (Figs. 4a and e; 5 a and e; Tables 3 and 4). There were single studies reporting the predictive value of FA from DTI in GBM treatment follow-up [43]. Thus, the survival advantage of lower MK and higher MD values from DKI in diffuse glioma are novel findings.

In the context of the integrated diagnostic approach of 2016 CNS WHO [3], there was no significant difference between patients with different MK and MD values among the groups of IDH_{mut} AS, IDH_{wt} GBM, and $OD_{1p/19q\text{-}LOH}$. These results so far correspond to the findings

Table 3
Univariate Cox proportional hazards model for overall and progression-free survival in diffuse glioma.

Variable	n	Hazard Ratio (95% CI)	p value[1]	Hazard Ratio (95% CI)	p value[1]
		overall survival		progression-free survival	
Age	77	1.051 (1.017 – 1.087)[2]	0.004	1.032 (1.017 – 1.087)[2]	0.004
WHO grade					
grade II	33	Reference		Reference	
grade III	21	8.299 (1.759 – 39.145)	0.007	1.701 (1.645 – 10.668)	0.007
grade IV	23	16.619 (2.943 – 93.849)	0.001	7.661 (2.884 – 20.352)	0.001
IDH1/2					
IDH1/2 wild type	39	Reference		Reference	
IDH1/2 mutation	38	0.067 (0.015 – 0.302)	<0.0001	0.168 (0.074 – 0.380)	<0.0001
ATRX					
ATRX loss	20	Reference		Reference	
ATRX retention	57	3.510 (0.792 – 15.561)	0.098	2.881 (1.098 – 7.557)	0.032
Resection status					
Biopsy	22	Reference		Reference	
Partial resection	13	1.002 (0.300 – 3.344)	0.998	0.664 (0.310 – 2.110)	0.664
Subtotal resection	33	0.113 (0.024 – 0.524)	0.005	0.367 (0.162 – 0.830)	0.016
Complete resection	9	0.189 (0.024 – 1.499)	0.115	0.209 (0.047 – 0.922)	0.039
Mean Kurtosis[3]					
average	77	40.499 (2.061 – 795.679)	0.015	50.753 (6.190 – 416.125)	<0.0001
standard deviation	77	17.624 (0.003 – 89318)	0.510	853.500 (1.5 – 480532.0)	0.037
skewness	77	0.689 (0.485 – 0.979)	0.037	0.799 (0.635 – 1.004)	0.054
kurtosis	77	0.972 (0.920 – 1.027)	0.305	0.992 (0.977 – 1.007)	0.287
mode	77	35.651 (1.392 – 913.330)	0.031	23.470 (2.543 – 216.615)	0.005
10th centile	77	110.933 (3.096 – 3975)	0.010	65.960 (5.582 – 779.471)	0.001
25th centile	77	48.484 (2.198 – 1069)	0.014	42.261 (4.856 – 367.788)	0.001
50th centile	77	37.925 (2.083 – 690.379)	0.014	41.890 (5.443 – 322.364)	<0.0001
75th centile	77	21.148 (1.769 – 252.770)	0.016	33.909 (5.261 – 218.548)	<0.0001
90th centile	77	12.118 (1.477 –99.422)	0.020	32.787 (5.750 –186.952)	<0.0001
Mean Diffusivity[3,4]					
average	77	0.239 (0.050 – 1.136)	0.072	0.210 (0.065 – 0.673)	0.009
standard deviation	77	16.909 (0.082 – 3491)	0.298	166.094 (2.774 – 9945)	0.014
skewness	77	1.289 (0.902 – 1.841)	0.163	1.178 (0.906 – 1.533)	0.222
kurtosis	77	0.994 (0.897 – 1.101)	0.902	0.962 (0.882 – 1.051)	0.393
mode	77	0.481 (0.187 – 1.233)	0.127	0.351 (0.177 – 0.693)	0.003
10th centile	77	0.186 (0.035 – 0.995)	0.049	0.094 (0.024 – 0.368)	0.001
25th centile	77	0.185 (0.036 – 0.946)	0.043	0.131 (0.037 – 0.465)	0.002
50th centile	77	0.219 (0.047 – 1.024)	0.054	0.207 (0.067 – 0.639)	0.006
75th centile	77	0.279 (0.067 – 1.172)	0.081	0.299 (0.107 – 0.839)	0.022
90th centile	77	0.420 (0.112 – 1.570)	0.197	0.497 (0.189 – 1.306)	0.156

[1]Significant results (Wald test) at $\alpha < 0.05$ are highlighted in light blue. [2] The hazard ratio is for each 1-year increase in age. [3] The hazard ratio is for each 1-unit increase in mean kurtosis and mean diffusivity. [4] The unit for Mean Diffusivity values is s/mm^2.
Isocitrate-dehydrogenase (IDH) 1/2 mutation status; alpha-thalassemia/mental retardation syndrome X-linked (ATRX) loss of expression; O6-methylguanine DNA methyltransferase (MGMT) promoter methylation status;

of Latysheva et al. [44], who found that "apparent diffusion coefficient parameters […] did not stratify progression-free survival and overall survival […] in patients with oligodendrogliomas". Conversely, patients with lower MK and higher MD values showed significant better overall and progression-free survival among gliomas without chromosome 1p/19q LOH and those with retained ATRX expression, respectively (Figs. 4c—d and g–h; 5c—d and g–h). The survival advantage of lower MK and higher MD values from DKI in theses glioma subgroups are novel findings. In the group of IDH_{wt} GBM we observed a statistic trend towards better overall and progression-free survival in patients with lower MK and higher MD values. MK and MD from DKI may predict the molecular profile of diffuse glioma [25,37]. Histogram analyses from DKI parameters have shown specific histogram types of the different molecular glioma groups [26] and indicated a more homogeneous distribution of DKI histogram parameters in the groups of IDH_{mut} AS and $OD_{1p/19q\text{-}LOH}$, whereas the group of IDH_{wt} GBM showed heterogeneous histogram parameter distribution. In this study we observe different survival, based on MK and MD stratification, in the gliomas with ATRX retention, which is characteristic of IDH_{wt} GBM. This indicates that the heterogeneous group of IDH_{wt} GBM shows different survival based on the individual complexity and heterogeneity of a tumor. Regarding the Kaplan-Meier plots (Figs. 4b and 5 b) the survival advantage in these groups might become significant in a bigger cohort.

Regarding the different DKI parameters we found that MK performed better than MD in predicting survival on preoperative images. These findings so far correspond to previous reports [26], where MK histogram parameters performed better than those of MD in non-invasively predicting the integrated molecular glioma profile. We did not find corresponding values in the literature.

Table 4
Preoperative multivariate Cox proportional hazards model for overall and progression-free survival in diffuse glioma.

Variable	n	Hazard Ratio (95% CI)	p value[1]	Hazard Ratio (95% CI)	p value[1]
		overall survival		progression-free survival	
Age	77	1.049 (1.012 – 1.088)[2]	0.010	1.028 (1.004 – 1.053)[2]	0.021
Mean Kurtosis					
average	77	22.764 (1.065 – 486.632)[3]	0.045	36.744 (4.277 – 315.662)[3]	0.001

[1] Significant results (Wald test) at $\alpha < 0.05$ are highlighted in light blue.
[2] The hazard ratio is for each 1-year increase in age.
[3] The hazard ratio is for each 1-unit increase in mean kurtosis.

In multivariate Cox proportional hazards analysis, both age and average MK are significant prognostic factors in preoperative setting. However, DKI parameters may not hold up with histopathologic or molecular glioma features. This partially supports previous findings, where contrast enhancement as a preoperative MR imaging feature was no longer prognostic in multivariate analysis including histopathologic and molecular markers [40].

6. Limitations

The relatively small numbers of patients with IDH_{mut} GBM and IDH_{wt} AS2 (early precursor lesion of IDH_{wt} GBM with evidence of possible emersion into a new midline high grade glioma subset in approx. 8% of IDH_{wt} AS [6]) might induce potential selection bias and did not allow for a deeper subgroup survival analysis. However, the distribution of our glioma cases represents their natural incidence [6,7,9,12,45]. Furthermore, there was potential treatment bias on the survival due to the different chemotherapy approaches adapted to the molecular glioma profile. Final limitation is the retrospective study design.

7. Conclusions

As isolated factors, patient age and average MK from DKI are relevant for predicting overall and progression-free survival in diffuse glioma on preoperative MRI scans. Regarding the different integrated molecular subgroups, MK and MD might be predictive factors in gliomas with retained ATRX expression, which is a characteristic of IDH_{wt} GBM. However, in this specific group the prognostic value of DKI parameters needs to be evaluated in a bigger cohort.

Conflicts of interest

The authors declare no conflict of interest. The founding sponsors had no role in the design of the study; in the collection, analyses, or interpretation of data; in the writing of the manuscript, and in the decision to publish the results.

Acknowledgements

We thank Mrs. Aline Naumann from the Institute of Clinical Epidemiology and Applied Biometry of the Eberhard Karls University of Tübingen for her support in statistics. JS was supported by the Else-Übelmesser Foundation (grant no. 30.19845).

References

[1] M. Weller, M. van den Bent, J.C. Tonn, R. Stupp, M. Preusser, E. Cohen-Jonathan-Moyal, et al., European Association for Neuro-Oncology (EANO) guideline on the diagnosis and treatment of adult astrocytic and oligodendroglial gliomas, Lancet Oncol. 18 (2017) e315–e329, https://doi.org/10.1016/S1470-2045(17)30194-8.

[2] J. Schittenhelm, Recent advances in subtyping tumors of the central nervous system using molecular data, Expert Rev. Mol. Diagn. 17 (2017) 83–94, https://doi.org/10.1080/14737159.2017.1266259.

[3] D.N. Louis, A. Perry, G. Reifenberger, Deimling A. von, D. Figarella-Branger, W.K. Cavenee, et al., The 2016 world health organization classification of tumors of the central nervous system: a summary, Acta Neuropathol. (131) (2016) 803–820, https://doi.org/10.1007/s00401-016-1545-1.

[4] J.N. Scott, P.M.A. Brasher, R.J. Sevick, N.B. Rewcastle, P.A. Forsyth, How often are nonenhancing supratentorial gliomas malignant? A population study, Neurology 59 (2002) 947–949.

[5] M. Watanabe, R. Tanaka, N. Takeda, Magnetic resonance imaging and histopathology of cerebral gliomas, Neuroradiology 34 (1992) 463–469.

[6] D.E. Reuss, A. Kratz, F. Sahm, D. Capper, D. Schrimpf, C. Koelsche, et al., Adult IDH wild type astrocytomas biologically and clinically resolve into other tumor entities, Acta Neuropathol. 130 (2015) 407–417, https://doi.org/10.1007/s00401-015-1454-8.

[7] D.E. Reuss, Y. Mamatjan, D. Schrimpf, D. Capper, V. Hovestadt, A. Kratz, et al., IDH mutant diffuse and anaplastic astrocytomas have similar age at presentation and little difference in survival: a grading problem for WHO, Acta Neuropathol. 129 (2015) 867–873, https://doi.org/10.1007/s00401-015-1438-8.

[8] F. Sahm, D. Reuss, C. Koelsche, D. Capper, J. Schittenhelm, S. Heim, et al., Farewell to oligoastrocytoma: in situ molecular genetics favor classification as either oligodendroglioma or astrocytoma, Acta Neuropathol. 128 (2014) 551–559, https://doi.org/10.1007/s00401-014-1326-7.

[9] D.E. Reuss, F. Sahm, D. Schrimpf, B. Wiestler, D. Capper, C. Koelsche, et al., ATRX and IDH1-R132H immunohistochemistry with subsequent copy number analysis and IDH sequencing as a basis for an "“integrated"” diagnostic approach for adult astrocytoma, oligodendroglioma and glioblastoma, Acta Neuropathol. 129 (2015) 133–146, https://doi.org/10.1007/s00401-014-1370-3.

[10] A. Olar, K.M. Wani, K.D. Alfaro-Munoz, L.E. Heathcock, H.F. van Thuijl, M.R. Gilbert, et al., IDH mutation status and role of WHO grade and mitotic index in overall survival in grade II-III diffuse gliomas, Acta Neuropathol. 129 (2015) 585–596, https://doi.org/10.1007/s00401-015-1398-z.

[11] M. Pekmezci, T. Rice, A.M. Molinaro, K.M. Walsh, P.A. Decker, H. Hansen, et al., Adult infiltrating gliomas with WHO 2016 integrated diagnosis: additional prognostic roles of ATRX and TERT // adult infiltrating gliomas with WHO 2016 integrated diagnosis: additional prognostic roles of ATRX and TERT, Acta Neuropathol. (133) (2017) 1001–1016, https://doi.org/10.1007/s00401-017-1690-1.

[12] H. Suzuki, K. Aoki, K. Chiba, Y. Sato, Y. Shiozawa, Y. Shiraishi, et al., Mutational landscape and clonal architecture in grade II and III gliomas, Nat. Genet. 47 (2015) 458–468, https://doi.org/10.1038/ng.3273.

[13] A. Ebrahimi, M. Skardelly, I. Bonzheim, I. Ott, H. Muhleisen, F. Eckert, et al., ATRX immunostaining predicts IDH and H3F3A status in gliomas, Acta Neuropathol. Commun. 4 (2016) 60, https://doi.org/10.1186/s40478-016-0331-6.

[14] M. Abedalthagafi, J.J. Phillips, G.E. Kim, S. Mueller, D.A. Haas-Kogen, R.E. Marshall, et al., The alternative lengthening of telomere phenotype is significantly associated with loss of ATRX expression in high-grade pediatric and adult astrocytomas: a multi-institutional study of 214 astrocytomas, Mod. Pathol. 26 (2013) 1425–1432, https://doi.org/10.1038/modpathol.2013.90.

[15] M.E. Hegi, A.-C. Diserens, T. Gorlia, M.-F. Hamou, Tribolet N. de, M. Weller, et al., MGMT gene silencing and benefit from temozolomide in glioblastoma, N. Engl. J. Med. 352 (2005) 997–1003, https://doi.org/10.1056/NEJMoa043331.

[16] M.J. van den Bent, B. Baumert, S.C. Erridge, M.A. Vogelbaum, A.K. Nowak, M. Sanson, et al., Interim results from the CATNON trial (EORTC study 26053-22054) of treatment with concurrent and adjuvant temozolomide for 1p/19q non-co-deleted anaplastic glioma: a phase 3, randomised, open-label intergroup study, Lancet 390 (2017) 1645–1653, https://doi.org/10.1016/S0140-6736(17)31442-3.

[17] R. Stupp, W.P. Mason, M.J. van den Bent, M. Weller, B. Fisher, M.J.B. Taphoorn, et al., Radiotherapy plus concomitant and adjuvant temozolomide for glioblastoma, N. Engl. J. Med. 352 (2005) 987–996, https://doi.org/10.1056/NEJMoa043330.

[18] A.V. Kulkarni, A. Guha, A. Lozano, M. Bernstein, Incidence of silent hemorrhage and delayed deterioration after stereotactic brain biopsy, J. Neurosurg. 89 (1998) 31–35, https://doi.org/10.3171/jns.1998.89.1.0031.

[19] J.H. Jensen, J.A. Helpern, MRI quantification of non-Gaussian water diffusion by kurtosis analysis, NMR Biomed. 23 (2010) 698–710, https://doi.org/10.1002/nbm.1518.

[20] J.H. Jensen, J.A. Helpern, A. Ramani, H. Lu, K. Kaczynski, Diffusional kurtosis imaging: the quantification of non-gaussian water diffusion by means of magnetic resonance imaging, Magn. Resonan. Med. 53 (2005) 1432–1440, https://doi.org/10.1002/mrm.20508.

[21] A.B. Rosenkrantz, A.R. Padhani, T.L. Chenevert, D.-M. Koh, Keyzer F de, B. Taouli, D. Le Bihan, Body diffusion kurtosis imaging: basic principles, applications, and considerations for clinical practice, J. Magn. Reson. Imaging 42 (2015) 1190–1202, https://doi.org/10.1002/jmri.24985.

[22] H. Lu, J.H. Jensen, A. Ramani, J.A. Helpern, Three-dimensional characterization of non-gaussian water diffusion in humans using diffusion kurtosis imaging, NMR Biomed. 19 (2006) 236–247, https://doi.org/10.1002/nbm.1020.

[23] J.H. Jensen, J.A. Helpern, A. Tabesh, Leading non-Gaussian corrections for diffusion orientation distribution function, NMR Biomed. 27 (2014) 202–211.

[24] D.H.J. Poot, A.J. den Dekker, E. Achten, M. Verhoye, J. Sijbers, Optimal experimental design for diffusion kurtosis imaging, IEEE Trans. Med. Imaging 29 (2010) 819–829, https://doi.org/10.1109/TMI.2009.2037915.

[25] J.-M. Hempel, S. Bisdas, J. Schittenhelm, C. Brendle, B. Bender, H. Wassmann, et al., In vivo molecular profiling of human glioma using diffusion kurtosis imaging, J. Neurooncol. 131 (2017) 93–101, https://doi.org/10.1007/s11060-016-2272-0.

[26] J.-M. Hempel, J. Schittenhelm, C. Brendle, B. Bender, G. Bier, M. Skardelly, et al., Histogram analysis of diffusion kurtosis imaging estimates for in vivo assessment of 2016 WHO glioma grades: a cross-sectional observational study, Eur. J. Radiol. (95) (2017) 202–211, https://doi.org/10.1016/j.ejrad.2017.08.008.

[27] Elm E. von, D.G. Altman, M. Egger, S.J. Pocock, P.C. Gøtzsche, J.P. Vandenbroucke, The strengthening the reporting of observational studies in epidemiology (STROBE) statement: guidelines for reporting observational studies, J. Clin. Epidemiol. 61 (2008) 344–349, https://doi.org/10.1016/j.jclinepi.2007.11.008.

[28] D. Capper, S. Weissert, J. Balss, A. Habel, J. Meyer, D. Jager, et al., Characterization of R132H mutation-specific IDH1 antibody binding in brain tumors, Brain Pathol. 20 (2010) 245–254, https://doi.org/10.1111/j.1750-3639.2009.00352.x.

[29] C. Hartmann, J. Meyer, J. Balss, D. Capper, W. Mueller, A. Christians, et al., Type and frequency of IDH1 and IDH2 mutations are related to astrocytic and oligodendroglial differentiation and age: a study of 1,010 diffuse gliomas, Acta Neuropathol. 118 (2009) 469–474, https://doi.org/10.1007/s00401-009-0561-9.

[30] N. Thon, S. Eigenbrod, E.M. Grasbon-Frodl, M. Ruiter, J.H. Mehrkens, S. Kreth, et al., Novel molecular stereotactic biopsy procedures reveal intratumoral homogeneity of loss of heterozygosity of 1p/19q and TP53 mutations in World Health Organization grade II gliomas, J. Neuropathol. Exp. Neurol. 68 (2009) 1219–1228, https://doi.org/10.1097/NEN.0b013e3181bee1f1.

[31] S.L. Gerson, MGMT: its role in cancer aetiology and cancer therapeutics, Nat. Rev. Cancer 4 (2004) 296–307, https://doi.org/10.1038/nrc1319.
[32] D.J. Tozer, H.R. Jäger, N. Danchaivijitr, C.E. Benton, P.S. Tofts, J.H. Rees, A.D. Waldman, Apparent diffusion coefficient histograms may predict low-grade glioma subtype, NMR Biomed. 20 (2007) 49–57, https://doi.org/10.1002/nbm.1091.
[33] J.-M. Hempel, J. Schittenhelm, S. Bisdas, C. Brendle, B. Bender, G. Bier, et al., In vivo assessment of tumor heterogeneity in WHO 2016 glioma grades using diffusion kurtosis imaging: diagnostic performance and improvement of feasibility in routine clinical practice, J. Neuroradiol. (45) (2018) 32–40, https://doi.org/10.1016/j.neurad.2017.07.005.
[34] R.E. Tarone, J. Ware, On distribution-free tests for equality of survival distributions, Biometrika 64 (1977) 156–160, https://doi.org/10.1093/biomet/64.1.156.
[35] G. Bouliotis, L. Billingham, Crossing survival curves: alternatives to the log-rank test, Trials 12 (2011), https://doi.org/10.1186/1745-6215-12-S1-A137 A137.
[36] S. Popov, A. Jury, R. Laxton, L. Doey, N. Kandasamy, S. Al-Sarraj, et al., IDH1-associated primary glioblastoma in young adults displays differential patterns of tumour and vascular morphology, PLoS One 8 (2013), https://doi.org/10.1371/journal.pone.0056328 e56328.
[37] J. Zhao, Y.-L. Wang, X.-B. Li, M.-S. Hu, Z.-H. Li, Y.-K. Song, et al., Comparative analysis of the diffusion kurtosis imaging and diffusion tensor imaging in grading gliomas, predicting tumour cell proliferation and IDH-1 gene mutation status, J. Neurooncol. (2018), https://doi.org/10.1007/s11060-018-03025-7.
[38] M. Lacroix, D. Abi-Said, D.R. Fourney, Z.L. Gokaslan, W. Shi, F. DeMonte, et al., A multivariate analysis of 416 patients with glioblastoma multiforme: prognosis, extent of resection, and survival, J. Neurosurg. 95 (2001) 190–198, https://doi.org/10.3171/jns.2001.95.2.0190.
[39] Y.Y. Wang, K. Wang, S.W. Li, J.F. Wang, J. Ma, T. Jiang, J.P. Dai, Patterns of tumor contrast enhancement predict the prognosis of anaplastic gliomas with IDH1 mutation, AJNR Am. J. Neuroradiol. 36 (2015) 2023–2029, https://doi.org/10.3174/ajnr.A4407.
[40] J.-M. Hempel, C. Brendle, B. Bender, G. Bier, M. Skardelly, I. Gepfner-Tuma, et al., Contrast enhancement predicting survival in integrated molecular subtypes of diffuse glioma: an observational cohort study, J. Neurooncol. 139 (2018) 373–381, https://doi.org/10.1007/s11060-018-2872-y.
[41] A. Hilario, J.M. Sepulveda, A. Perez-Nunez, E. Salvador, J.M. Millan, A. Hernandez-Lain, et al., A prognostic model based on preoperative MRI predicts overall survival in patients with diffuse gliomas, AJNR Am. J. Neuroradiol. 35 (2014) 1096–1102, https://doi.org/10.3174/ajnr.A3837.
[42] Y. Cui, L. Ma, X. Chen, Z. Zhang, H. Jiang, S. Lin, Lower apparent diffusion coefficients indicate distinct prognosis in low-grade and high-grade glioma, J. Neurooncol. 119 (2014) 377–385, https://doi.org/10.1007/s11060-014-1490-6.
[43] T. Huber, S. Bette, B. Wiestler, J. Gempt, J. Gerhardt, C. Delbridge, et al., Fractional anisotropy correlates with overall survival in glioblastoma, World Neurosurg. 95 (2016) 525–534, https://doi.org/10.1016/j.wneu.2016.08.055 e1.
[44] A. Latysheva, K. Eeg Emblem, A. Server, P. Brandal, T.R. Meling, J. Pahnke, J.K. Hald, Survival associations using perfusion and diffusion magnetic resonance imaging in patients with histologic and genetic defined diffuse glioma world health organization grades II and III, J. Comput. Assist. Tomogr. (2018), https://doi.org/10.1097/RCT.0000000000000742.
[45] D. Unruh, S.R. Schwarze, L. Khoury, C. Thomas, M. Wu, L. Chen, et al., Mutant IDH1 and thrombosis in gliomas, Acta Neuropathol. 132 (2016) 917–930, https://doi.org/10.1007/s00401-016-1620-7.